

Curved orogenic belts, back-arc basins, and obduction as consequences of collision at irregular continental margins

Nicholas Schliffke¹, Jeroen van Hunen¹, Frédéric Gueydan², Valentina Magni³ and Mark B. Allen¹

¹Department of Earth Sciences, Durham University, DH1 3LE Durham, UK

²Géosciences Montpellier, Université Montpellier 2, Place Eugène Bataillon, 34095 Montpellier cedex 5, France

³The Centre for Earth Evolution and Dynamics (CEED), University of Oslo, SemSaelandsvei 24, P.O. Box 1048, Blindern, NO-0316 Oslo, Norway

ABSTRACT

Continental collisions commonly involve highly curved passive plate margins, leading to diachronous continental subduction during trench rollback. Such systems may feature back-arc extension and ophiolite obduction postdating initial collision. Modern examples include the Alboran and Banda arcs. Ancient systems include the Newfoundland and Norwegian Caledonides. While external forces or preexisting weaknesses are often invoked, we suggest that ophiolite obduction can equally be caused by internal stress buildup during collision. Here, we modeled collision with an irregular subducting continental margin in three-dimensional (3-D) thermo-mechanical models and used the generated stress field evolution to understand resulting geologic processes. Results show how tensional stresses are localized in the overriding plate during the diachronous onset of collision. These stresses thin the overriding plate and may open a back-arc spreading center. Collision along the entire trench follows rapidly, with inversion of this spreading center, ophiolite obduction, and compression in the overriding plate. The models show how subduction of an irregular continental margin can form a highly curved orogenic belt. With this mechanism, obduction of back-arc oceanic lithosphere naturally evolves from a given initial margin geometry during continental collision.

INTRODUCTION

The formation of highly curved orogenic belts is still debated (Rosenbaum, 2014). Proposed mechanisms include processes associated with deformation along thinned fold-and-thrust belts (Marshak, 1988), gravitational spreading (e.g., Edey et al., 2020), or along-strike migration rate variations of plate boundaries (Rosenbaum and Lister, 2004). The latter includes processes such as plate rotation, trench rollback, or indentation during continental collision (Rosenbaum, 2014; Rosenbaum and Lister, 2004).

The Alboran and Banda arcs are two modern systems that are associated with trench rollback and diachronous continental subduction along strike (Spakman and Hall, 2010; van Hinsbergen et al., 2014). Both regions experienced trench rollback against a highly nonlinear passive margin (see Fig. 1), where continental lithosphere subducted diachronously along the trench (Pownall et al., 2016; Spakman and Hall, 2010; van Hinsbergen et al., 2014). In the Banda region, continental material initially (15 Ma) subducted at Seram (Spakman and Hall, 2010),

coinciding with trench rotation, and this was followed by continental subduction (4 Ma) at Timor, in the south (Fig. 1A). Oceanic subduction is now ceased, with collision occurring along the entire continental margin. The tectonic history of the Alboran Basin in the western Mediterranean is debated (van Hinsbergen et al., 2014). Most models agree that the slab retreated westward into the narrowing Alboran embayment since 30–20 Ma (Fig. 1B).

Both regions share puzzling geological features, such as extensional basins in the upper plate (Pownall et al., 2016; Watts et al., 1993), and exhumed subcrustal continental lithosphere (Frasca et al., 2017; Gueydan et al., 2019; Pownall et al., 2014). The Banda system involves ophiolite obduction (Ishikawa et al., 2007), but this has not been identified in the Alboran arc. The world's largest subcontinental mantle exposures, the Ronda and Beni peridotites in the Alboran arc (Gueydan et al., 2019), have been suggested to have been exhumed by gravitational collapse after slab break-off (Platt and Vissers, 1989; Van der Wal and Vissers, 1993),

by thrusting of an older Jurassic rifted margin (Tubia et al., 2009), or by hyperextension of the overriding plate before, and thrusting during, continental collision (Frasca et al., 2017; Gueydan et al., 2019; see Fig. 1C). It is unclear in these examples how the geologic evolution is linked to the highly arcuate geometry and irregular shape of the subducting continental margin, if at all.

The aim of this study was to examine evolving plate stresses during irregular continental subduction and the formation of curved orogenic belts, to provide a better understanding of the drivers and controls of the geologic evolution. We show that localized tensional stresses during the initial stages of irregular margin collision cause short-lived back-arc rifting or spreading centers that are rapidly inverted once continental subduction spreads along the trench.

COLLISION WITH IRREGULAR PASSIVE MARGINS

We investigated the stress regime evolution during continental collision with an irregular margin (Fig. 2) in a model space of 3300 by 3960 by 660 km in size. The finite element code Citcom (Moresi et al., 1996; Zhong et al., 2000; Magni et al., 2014) solves the conservation equations for momentum, energy, mass, and composition. We used a visco-plastic rheology including diffusion and dislocation creep, lithospheric yielding, and an upper-limit viscosity (Magni et al., 2014; van Hunen and Allen, 2011). We did not apply external forcing; all dynamics were driven by internal buoyancy forces. Subducting and overriding plates were separated by a weak zone and decoupled from neighboring plates by weak transform faults to permit toroidal mantle flow (van Hunen and Allen, 2011; Magni et al., 2014). Continental lithosphere was free to move toward the trench and collide with the overriding

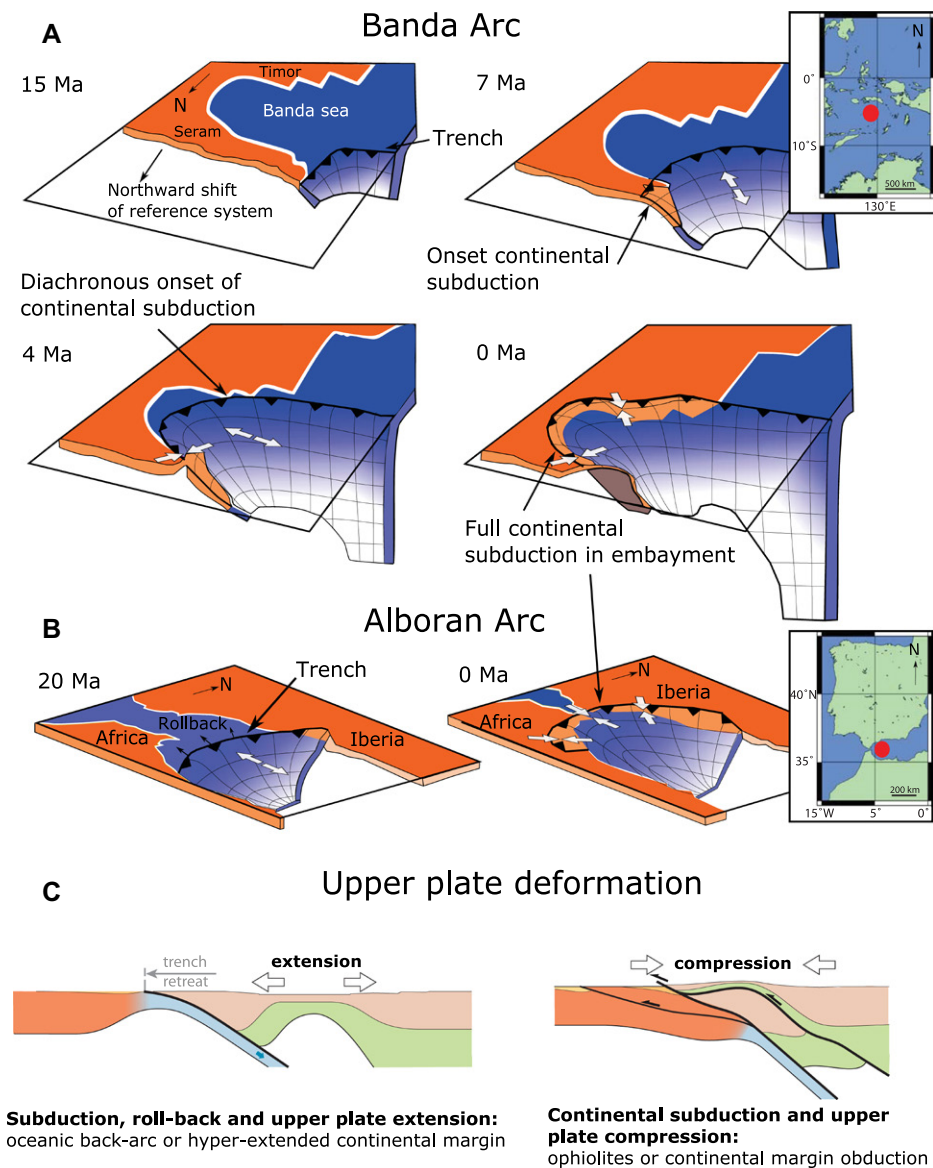


Figure 1. (A–B) Tectonic history of Banda (A) and Alboran (B) systems with diachronous continental subduction and trench rollback before continental subduction along entire trench ended subduction (overriding plate not shown in A–B). Orange—continental domains; blue—oceanic domains. (C) Mechanism for hyperextended margin obduction in Alboran domain (based on Gueydan et al., 2019), with extension in overriding plate predating continental subduction.

plate as the intervening oceanic basin closed. The continental crust was initially 40 km thick; the underlying mantle lithosphere extended from 100 km depth close to the trench to 150 km in the far-field area to mimic the thicker plate interior (Fig. 2B). The subducting passive margin included an oceanic embayment of (along-strike) width w_b and breadth (here used for the across-strike width) b_b , with flanks that sat at an angle α with respect to the convergence direction. To study the impact of this embayment on the evolving stress distribution, we varied the initial width (between 600 and 1200 km) and breadth (between 300 and 700 km) while keeping the flank orientation angle α constant. The convergence-parallel stress field, σ_{xx} , was computed to investigate the stress localization

that could be responsible for the observed normal or thrust faulting.

Figure 3 depicts the model evolution of a subducting continent including an oceanic embayment $w_b = 1000$ km by $b_b = 600$ km. Initially, negative buoyancy of the oceanic slab drives subduction, trench rollback, and uniform extension in the overriding plate in all models (Fig. 3A). Initial continental subduction at the sides of the embayment locally reduces subduction velocities, and trench retreat stops (Fig. 3B). Trench retreat continues, however, at the oceanic embayment on the passive margin. With the local onset of continental collision (Fig. 3B), stresses start to vary significantly along the trench and upper plate. There is localized compression in collision regions,

while extension close to the oceanic embayment continues to exert slab pull and trench retreat. The differential stresses cause yielding and rupture of the overriding plate. Opening of a back-arc spreading center (Fig. 3C) briefly increases convergence velocities by a factor of three (Fig. 4A). Shortly (~ 5 m.y.) after onset of back-arc spreading, the oceanic embayment is completely subducted, and this is followed by continental subduction (Figs. 3D–3F). At this point, the young oceanic back-arc basin measures only 166 km in ridge-perpendicular spreading distance (Fig. 3D). High continental crustal buoyancy reduces subduction velocities and stops trench rollback (Fig. 4A). Without local, rapid trench rollback driving the extensional stresses in the back-arc area, back-arc spreading ceases, and its stress state changes from an extensional to a compressional stress state within 10 m.y. after initial collision (Figs. 3E and 3F). During this last stage, slab break-off along the entire subducted margin ends subduction and allows the subducted continent to begin exhumation.

Subduction of smaller embayments (Fig. 4B) does not rupture the overriding plate to produce back-arc spreading, but it still thins the overriding continent; crustal thickness reduces from the initial 40 km to as little as 8 km (Fig. 4B; Fig. S1 in the Supplemental Material¹) at the onset of collision. The embayment breadth, b_b , determines the duration of the overriding plate extensional phase, and hence the presence or absence of an oceanic back-arc basin. Too narrow embayments (small w_b) do not create sufficient tensional stresses, while the widest embayments ($w_b = 1200$ km) lack the required stress localization. When a back-arc spreading center is formed, its spreading duration varies from 1 m.y. in the smallest basin, to 5 m.y. (reference model, Fig. 3), to 10 m.y. in the models with the largest embayments ($w_b = 1200$ km and $b_b = 600$ km) and forming the largest back-arc basin (253 km cross-spreading distance).

DISCUSSION AND CONCLUSION

Subduction of an irregular passive margin allows formation of curved orogenic belts and a two-stage stress evolution from extensional to compressional states in the overriding plate during collision. Our models show how localized thinning or rupturing of the overriding plate occurs during local initial collision, while oceanic subduction continues elsewhere. Stress inversion and compressional deformation take place in a second stage, during full continental

¹Supplemental Material. Detailed figures of the model evolution, as well as a short description of the methodology and parameters used. Please visit <https://doi.org/10.1130/GEOLOGY.S15062262> to access the supplemental material, and contact editing@geosociety.org with any questions.

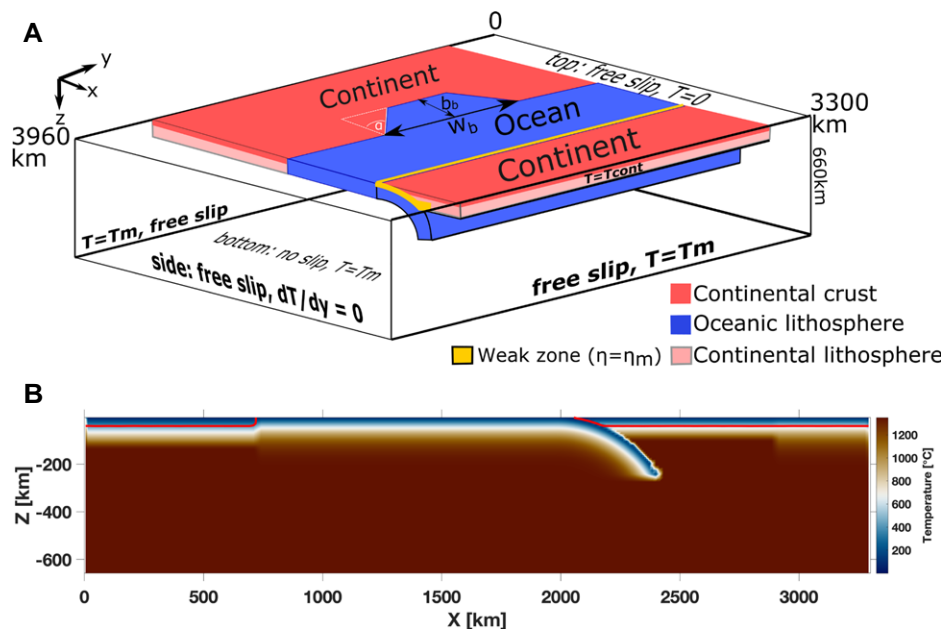


Figure 2. (A) Model setup: continental margin contains an oceanic embayment of breadth b_b and width w_b , and collides with continental overriding plate after closure of oceanic basin. Overriding plate is fixed to right model boundary. Converging plates are decoupled by fixed-viscosity weak zone (yellow). See methodology for details. (B) Temperature (T) x-z cross section through center of model, with continental crust outlined in red. T_m —mantle temperature.

subduction. Such features are probably common in collision zones, given the naturally irregular shape of passive margins (Dewey and Burke, 1974).

Many numerical models of continental collision have focused on linear passive margins (Schliffke et al., 2019; van Hunen and Allen, 2011) or oblique collision (Bottrill et al., 2014) to study slab break-off and exhumation of subducted continental crust. Compressional stresses and resulting topography during continental collision are controlled by plate coupling (Faccenda et al., 2009), rheological flow laws (Pusok et al., 2018), and buoyancy ratios and convergence velocities (Pusok and Kaus, 2015). Also, lateral compositional variations along strike on the subducting plate can trigger the formation of back-arc spreading centers (Magni et al., 2014; Menant et al., 2016), under the precondition of nonlinear rheology (Pusok et al., 2018). Our models combined these approaches and showed that the resulting stress inversion from extensional to compressional states in the back-arc basins is similar to sequences proposed for the obduction of ophiolites (Cawood and Suhr, 1992) or hyperextended continental

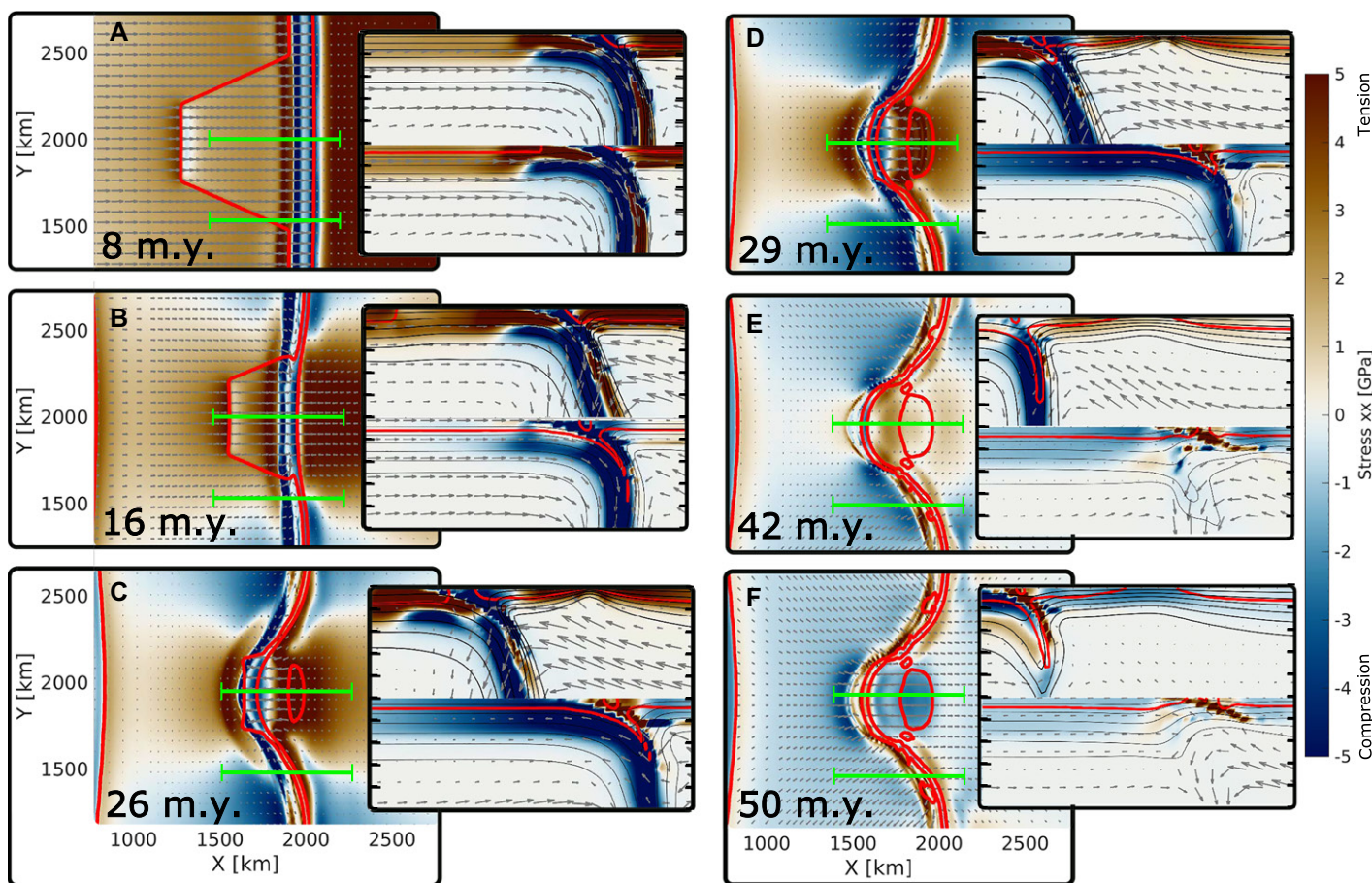


Figure 3. Stress evolution (σ_{xx}) at model surface with oceanic embayment measuring 1000 km by 600 km, where 250-km-deep vertical profiles are located at center and edge of embayment (green lines). Brown represents tension; blue is compression. Red contours outline continental crust; black lines are isotherms with 200 °C interval. Lateral onset of continental collision (A, B) triggers tensional stresses near embayment, opening back-arc basin (C, D). Once continental collision occurs within oceanic embayment, stresses in back-arc basin are inverted to shortening (E, F).

- Bay of Islands Complex, western Newfoundland: *Tectonics*, v. 11, p. 884–897, <https://doi.org/10.1029/92TC00471>.
- Dewey, J.F., and Burke, K., 1974, Hot spots and continental break-up: Implications for collisional orogeny: *Geology*, v. 2, p. 57–60, [https://doi.org/10.1130/0091-7613\(1974\)2<57:HSACBI>2.0.CO;2](https://doi.org/10.1130/0091-7613(1974)2<57:HSACBI>2.0.CO;2).
- Duretz, T., Agard, P., Yamato, P., Ducassou, C., Burov, E.B., and Gerya, T.V., 2016, Thermo-mechanical modeling of the obduction process based on the Oman ophiolite case: *Gondwana Research*, v. 32, p. 1–10, <https://doi.org/10.1016/j.jgr.2015.02.002>.
- Edey, A., Allen, M.B., and Nilfouroushan, F., 2020, Kinematic variation within the Fars arc, eastern Zagros, and the development of fold-and-thrust belt curvature: *Tectonics*, v. 39, p. e2019TC005941, <https://doi.org/10.1029/2019TC005941>.
- Faccenda, M., Minelli, G., and Gerya, T.V., 2009, Coupled and decoupled regimes of continental collision: Numerical modeling: *Earth and Planetary Science Letters*, v. 278, p. 337–349, <https://doi.org/10.1016/j.epsl.2008.12.021>.
- Frasca, G., Gueydan, F., Poujol, M., Brun, J.-P., Parat, F., Monié, P., et al., 2017, Fast switch from extensional exhumation to thrusting of the Ronda peridotites (south Spain): *Terra Nova*, v. 29, p. 117–126, <https://doi.org/10.1111/ter.12255>.
- Gueydan, F., Mazzotti, S., Tiberi, C., Cavin, R., and Villaseñor, A., 2019, Western Mediterranean subcontinental mantle emplacement by continental margin obduction: *Tectonics*, v. 38, p. 2142–2157, <https://doi.org/10.1029/2018TC005058>.
- Hassani, R., Jongmans, D., and Chéry, J., 1997, Study of plate deformation and stress in subduction processes using two-dimensional numerical models: *Journal of Geophysical Research: Solid Earth*, v. 102, B8, p. 17951–17965, <https://doi.org/10.1029/97JB01354>.
- Hässig, M., Rolland, Y., Duretz, T., and Sosson, M., 2016, Obduction triggered by regional heating during plate reorganization: *Terra Nova*, v. 28, p. 76–82, <https://doi.org/10.1111/ter.12193>.
- Ishikawa, A., Kaneko, Y., Kadarusman, A., and Ota, T., 2007, Multiple generations of forearc mafic-ultramafic rocks in the Timor–Tanimbar ophiolite, eastern Indonesia: *Gondwana Research*, v. 11, p. 200–217, <https://doi.org/10.1016/j.gr.2006.04.007>.
- Luth, S., Willingshofer, E., Sokoutis, D., and Cloetingh, S., 2010, Analogue modelling of continental collision: Influence of plate coupling on mantle lithosphere subduction, crustal deformation and surface topography: *Tectonophysics*, v. 484, p. 87–102, <https://doi.org/10.1016/j.tecto.2009.08.043>.
- Magni, V., Faccenna, C., van Hunen, J., and Funicello, F., 2014, How collision triggers backarc extension: Insight into Mediterranean style of extension from 3-D numerical models: *Geology*, v. 42, p. 511–514, <https://doi.org/10.1130/G35446.1>.
- Marshak, S., 1988, Kinematics of orocline and arc formation in thin-skinned orogens: *Tectonics*, v. 7, p. 73–86, <https://doi.org/10.1029/TC007i001p00073>.
- Menant, A., Sternai, P., Jolivet, L., Guillou-Frotier, L., and Gerya, T., 2016, 3D numerical modeling of mantle flow, crustal dynamics and magma genesis associated with slab roll-back and tearing: The eastern Mediterranean case: *Earth and Planetary Science Letters*, v. 442, p. 93–107, <https://doi.org/10.1016/j.epsl.2016.03.002>.
- Moresi, L., Zhong, S., and Gurnis, M., 1996, The accuracy of finite element solutions of Stokes's flow with strongly varying viscosity: *Physics of the Earth and Planetary Interiors*, v. 97, p. 83–94, [https://doi.org/10.1016/0031-9201\(96\)03163-9](https://doi.org/10.1016/0031-9201(96)03163-9).
- Platt, J.P., and Vissers, R.L.M., 1989, Extensional collapse of thickened continental lithosphere: A working hypothesis for the Alboran Sea and Gibraltar arc: *Geology*, v. 17, p. 540–543, [https://doi.org/10.1130/0091-7613\(1989\)017<0540:ECOTCL>2.3.CO;2](https://doi.org/10.1130/0091-7613(1989)017<0540:ECOTCL>2.3.CO;2).
- Pownall, J.M., Hall, R., Armstrong, R.A., and Forster, M.A., 2014, Earth's youngest known ultrahigh-temperature granulites discovered on Seram, eastern Indonesia: *Geology*, v. 42, p. 279–282, <https://doi.org/10.1130/G35230.1>.
- Pownall, J.M., Hall, R., and Lister, G.S., 2016, Rolling open Earth's deepest forearc basin: *Geology*, v. 44, p. 947–950, <https://doi.org/10.1130/G38051.1>.
- Pusok, A.E., and Kaus, B.J.P., 2015, Development of topography in 3-D continental-collision models: *Geochemistry Geophysics Geosystems*, v. 16, p. 1378–1400, <https://doi.org/10.1002/2015GC005732>.
- Pusok, A.E., Kaus, B.J.P., and Popov, A.A., 2018, The effect of rheological approximations in 3-D numerical simulations of subduction and collision: *Tectonophysics*, v. 746, p. 296–311, <https://doi.org/10.1016/j.tecto.2018.04.017>.
- Rosenbaum, G., 2014, Geodynamics of oroclinal bending: Insights from the Mediterranean: *Journal of Geodynamics*, v. 82, p. 5–15, <https://doi.org/10.1016/j.jog.2014.05.002>.
- Rosenbaum, G., and Lister, G.S., 2004, Formation of arcuate orogenic belts in the western Mediterranean region, *in* Sussman, A.J., and Weil, A.B., eds., *Orogenic Curvature: Integrating Paleomagnetic and Structural Analyses*: Geological Society of America Special Paper 383, p. 41–56, [https://doi.org/10.1130/0-8137-2383-3\(2004\)383\[41:FOAOBI\]2.0.CO;2](https://doi.org/10.1130/0-8137-2383-3(2004)383[41:FOAOBI]2.0.CO;2).
- Schliffke, N., van Hunen, J., Magni, V., and Allen, M.B., 2019, The role of crustal buoyancy in the generation and emplacement of magmatism during continental collision: *Geochemistry Geophysics Geosystems*, v. 20, p. 4693–4709, <https://doi.org/10.1029/2019GC008590>.
- Slagstad, T., and Kirkland, C.L., 2018, Timing of collision initiation and location of the Scandinavian orogenic suture in the Scandinavian Caledonides: *Terra Nova*, v. 30, p. 179–188, <https://doi.org/10.1111/ter.12324>.
- Spakman, W., and Hall, R., 2010, Surface deformation and slab-mantle interaction during Banda arc subduction rollback: *Nature Geoscience*, v. 3, p. 562, <https://doi.org/10.1038/ngeo917>.
- Tubia, J.M., Cuevas, J., Esteban, J.J., and Gil Ibarra, J.I., 2009, Remnants of a Mesozoic rift in a subducted terrane of the Alpujarride Complex (Betic Cordilleras, southern Spain): *The Journal of Geology*, v. 117, p. 71–87, <https://doi.org/10.1086/593322>.
- Van der Wal, D., and Vissers, R.L.M., 1993, Uplift and emplacement of upper mantle rocks in the western Mediterranean: *Geology*, v. 21, p. 1119–1122, [https://doi.org/10.1130/0091-7613\(1993\)021<1119:UAEOUM>2.3.CO;2](https://doi.org/10.1130/0091-7613(1993)021<1119:UAEOUM>2.3.CO;2).
- van Hinsbergen, D.J.J., Vissers, R.L.M., and Spakman, W., 2014, Origin and consequences of western Mediterranean subduction, rollback, and slab segmentation: *Tectonics*, v. 33, p. 393–419, <https://doi.org/10.1002/2013TC003349>.
- van Hunen, J., and Allen, M.B., 2011, Continental collision and slab break-off: A comparison of 3-D numerical models with observations: *Earth and Planetary Science Letters*, v. 302, p. 27–37, <https://doi.org/10.1016/j.epsl.2010.11.035>.
- Watts, A.B., Piatt, J.P., and Buhl, P., 1993, Tectonic evolution of the Alboran Sea basin: *Basin Research*, v. 5, p. 153–177, <https://doi.org/10.1111/j.1365-2117.1993.tb00063.x>.
- Zhong, S., Zuber, M.T., Moresi, L., and Gurnis, M., 2000, Role of temperature-dependent viscosity and surface plates in spherical shell models of mantle convection: *Journal of Geophysical Research: Solid Earth*, v. 105, B5, p. 11063–11082, <https://doi.org/10.1029/2000JB900003>.

Printed in USA